Synthesis, Chiroptical and Electrochemical Studies of Dioxouranium(VI) Complexes of Aldimine Derivatives of L-/D-Histidine and Crystal Structure of (2,2'-Bipyridyl)dioxo-(*N*-*o*-vanillylidene-L-histidinato)uranium(VI)–Water–Methanol(1/1/1)†

Subrata Panchanan,[a] Reijo Hämäläinen[b] and Parag S. Roy*[,a]

[a] *Department of Chemistry, University of North Bengal, Dist. Darjeeling-734 430, India*

[b] *Department of Chemistry, University of Helsinki, SF-00014 Helsinki, Finland*

A series of new dioxouranium(VI) complexes has been synthesised using *N*-(salicylidene)-L-histidine (H_2sal-L-his) and *N*-(*o*-vanillylidene)-L-histidine (H_2van-L-his) and the corresponding D-histidines. They have been characterized by elemental analyses and physicochemical studies. The crystal and molecular structures of $[UO_2(van\text{-}L\text{-}his)(bipy)]\cdot MeOH\cdot H_2O$ (bipy = 2,2'-bipyridine) have been determined by X-ray crystallography. The aldimine ligand in this compound is tridentate. The methanol and water molecules are hydrogen bonded to each other and the water molecule to the carboxylate O atom. The diamagnetic UO_2^{2+} entity serves as a chiroptical probe, undergoing stereospecific complex formation with the aldimine ligands, as well as for the interpretation of their ^1H NMR spectra, which in conjunction with two-dimensional NMR spectra, reveal the different spin-spin interactions, including the long range one between the azomethine (CH=N) and H_α proton of the amino acid residue. The CD and NMR spectral data of the quasi-enantiomorphous UO_2^{2+} complexes containing the L-/D-amino acid residues have helped to ascertain the conformational differences between each such pair; these differences can modulate energies of the half-filled highest occupied molecular orbitals in different ways. As these orbitals are involved in the electron-transfer process, the relevant complexes respond differently when subjected to cyclic voltammetry.

The different facets of the co-ordination compounds of first-series transition-metal ions with the aldimine derivatives of amino acids as well as of the ligands themselves have received considerable attention because of their relevance to various enzymatic (vitamin B_6 catalysed) and non-enzymatic model reactions of α-amino acids.[1-4] Such reactions, involving a number of electron and hydrogen shifts, are controlled mainly by subtle conformational effects around the N–C_α bond.[4,5]

X-Ray crystallographic studies on 1:1 (M:L) transition-metal complexes especially those of copper have shown that they are mostly bridged through the carboxylate oxygen atoms.[1,6,7] Another difficulty associated with the corresponding diamagnetic octahedral complexes of Al^{III} and Zn^{II} is the formation of several diastereoisomers with small energy differences, thereby complicating their NMR one-dimensional spectra.[1,2]

This work concerns the simplification/interpretation of two-dimensional NMR spectra of two sets of chelated chiral aldimine ligands derived from L-/D-histidine, using the diamagnetic UO_2^{2+} entity as a probe, since such studies are difficult for the corresponding paramagnetic systems.[8] Attention has also been focused, in the light of the salicylidenamino chirality rule, on the CD spectra of the complexes, in terms of contributions from configurational, conformational and vicinal factors.[3,9] These results help in monitoring the ligand conformational control of metal-centred electron-transfer reactions, using a temporal method like cyclic voltammetry.[10]

A modern trend in chiroptical studies on ligating natural products involves complex formation of the organic molecules with a metal cluster, in order to restrict the conformational freedom.[11] This stereochemical purpose has been achieved here, by utilizing the pentagonal/hexagonal planar co-ordination geometry of the UO_2^{2+} entity as a complex-forming matrix, for the pertinent aldimine ligands. The use of 2,2'-bipyridyl (bipy) and 1,10-phenanthroline (phen) as blocking agents affords the formation of mononuclear complexes. Histidine was chosen for obvious reasons, *e.g.* the histidyl residue is perhaps the most important metal-binding site in biological systems and histidine is present in a large number of enzyme active centres.[13]

Experimental

Materials.—*o*-Vanillin (2-hydroxy-3-methoxybenzaldehyde) (Fluka), salicylaldehyde (Kemphasol, India), L-histidine monohydrochloride monohydrate (E. Merck), D-histidine monohydrochloride monohydrate (Sigma), 2,2'-bipyridyl (BDH, India), 1,10-phenanthroline monohydrate (BDH, India) and uranyl nitrate hexahydrate (G.R.; Loba, Bombay) were used as such. Tetra-*n*-butylammonium perchlorate was prepared from tetra-*n*-butylammonium hydroxide (SISCO, Bombay).[14] The solvents were purified by literature procedures.[15]

Preparation of Ligands.—*Potassium* N-o-*vanillylidene*-L-*histidinate dihydrate* $K(Hvan\text{-}L\text{-}his)\cdot 2H_2O$ *and potassium* N-*salicylidene*-L-*histidinate* K(Hsal-L-his). These salts were synthesised by condensation of L-histidine monohydrochloride monohydrate (1 mmol) with *o*-vanillin or salicylaldehyde (1.25 mmol) in the presence of KOH (2 mmol) in methanol–water (7.5:1 v/v, 34 cm^3), followed by evaporation of the solvent. The dry mass was washed with diethyl ether, dissolved in dry methanol and the solvent removed *in vacuo*. The corresponding derivatives of D-histidine were prepared from D-histidine monohydrochloride monohydrate, following a similar procedure. Yields of these hygroscopic, orange-yellow to yellow

† *Supplementary data available:* see Instructions for Authors, *J. Chem. Soc., Dalton Trans.*, 1994, Issue 1, pp. xxiii–xxviii.

compounds were *ca.* 50–60%. Their purity was checked by elemental analyses {Found: C, 46.0; H, 4.6; N, 11.1 (L-derivative). C, 46.2; H, 4.8; N, 11.3 (D-derivative). Calc. for $C_{14}H_{14}N_3O_4K{\cdot}2H_2O$ [K(Hsal-L-/D-his)·$2H_2O$]: C, 46.3; H, 5.0; N, 11.6%. Found: C, 52.1; H, 3.7; N, 13.6 (L-derivative). C, 52.3; H, 3.9; N, 13.8 (D-derivative). Calc. for $C_{13}H_{12}N_3O_3K$ [K(Hsal-L-/D-his)]: C, 52.5; H, 4.0; N, 14.1%]}.

Preparation of the Complexes.—$K_2[UO_2(van\text{-}L\text{-}his)_2]{\cdot}4H_2O$ **1**. This complex was obtained by reacting *o*-vanillin (150 mg, 1 mmol) in methanol (5 cm^3) with a methanol–water (15 cm^3, 1:1 v/v) solution of L-histidine monohydrochloride monohydrate (210 mg, 1 mmol) in KOH (112 mg, 2 mmol), followed by reaction with $[UO_2(NO_3)_2]{\cdot}6H_2O$ (250 mg, 0.5 mmol) in methanol (5 cm^3). The reaction mixture was stirred for 0.5 h, followed by concentration to *ca.* 10 cm^3 on a steam-bath and then allowed to settle for 3 h. The precipitated compound was filtered off, washed with methanol–water (4:1 v/v), methanol, diethyl ether and dried over anhydrous $CaCl_2$ *in vacuo*.

$[UO_2(van\text{-}L\text{-}his)(bipy)]{\cdot}3H_2O$ **2**, $[UO_2(van\text{-}L\text{-}his)(phen)]{\cdot}H_2O$ **4**, $[UO_2(sal\text{-}L\text{-}his)(bipy)]{\cdot}2H_2O$ **5** and $[UO_2(sal\text{-}L\text{-}his)(phen)]{\cdot}4H_2O$ **6**. These complexes were prepared by a procedure involving formation of the ligands *in situ*, followed by reaction with 2,2′-bipyridyl or 1,10-phenanthroline monohydrate and $[UO_2(NO_3)_2]{\cdot}6H_2O$ in 1:1:1 molar proportion in methanol–water (4:1 v/v). For the *N*-(*o*-vanillylidene) complexes the amount of KOH was restricted to 56 mg (1 mmol), whereas for the other system a slight excess of KOH (84 mg, 1.5 mmol) had to be used.

$[UO_2(van\text{-}L\text{-}his)(bipy)]{\cdot}MeOH{\cdot}H_2O$ **3**. This complex was obtained by recrystallization of $[UO_2(van\text{-}L\text{-}his)(bipy)]{\cdot}3H_2O$ from methanol–water (4:1 v/v). The third recrystallization product was used for X-ray diffraction measurement.

The yields of these complexes were *ca.* 50–55%. They are slightly soluble in methanol, ethanol and moderately soluble in dimethylformamide and dimethyl sulfoxide. Apart from the template procedure described above, the complexes can also be synthesised in lower yields by reactions of the preformed ligands with $[UO_2(NO_3)_2]{\cdot}6H_2O$ under appropriate conditions. The characterization data for these complexes are shown in Table 4.

Direct reaction between $[UO_2(NO_3)_2]{\cdot}6H_2O$ and an aldimine ligand (1:2 molar ratio) in the absence of bipy or phen usually led to the formation of a dimeric complex, *e.g.* $[(UO_2)_2(sal\text{-}L\text{-}his)(Hsal\text{-}L\text{-}his)_2(H_2O)_2]{\cdot}4H_2O$ was obtained through the use of K(Hsal-L-his); this compound was characterized by elemental analysis, IR, UV/VIS and ^1H NMR spectra.

Physical Measurements.—The IR spectra on Nujol mull were recorded on a Philips Analytical SP3-300 spectrometer (4000–400 cm^{-1}) or in CsI on a Perkin-Elmer 983 spectrometer (4000–200 cm^{-1}). Electronic spectra in methanol were recorded on a Shimadzu (UV-240) spectrophotometer, CD spectra in methanol on a Jobin Yvon dichrograph RJ Mark III. The 300 MHz ^1H NMR spectra (one- and two-dimensional) in dimethyl sulfoxide were recorded on a Varian VXR 300 S spectrometer at 25 °C. Additional ^1H NMR spectra of some of the ligands were recorded (in D_2O) on a Varian XL-100 spectrometer. Electrochemical studies were performed with a Bioanalytical systems (BAS, U.S.A.) model CV-27 electroanalytical apparatus in Me_2SO–0.1 mol dm^{-3} $[NBu_4][ClO_4]$. The three-electrode (cyclic voltammetry, CV) measurements were carried out under a purified dinitrogen atmosphere in a gas-tight cell by using a BAS planar platinum-inlay working electrode, a platinum-wire auxiliary electrode and a saturated calomel electrode (SCE); the SCE was connected to the test solution through a Vycor tip. The reported potentials are uncorrected for junction contribution. Controlled-potential coulometric experiments (at 0.1–0.2 V past the cathodic peak potential of the respective CV diagram) were conducted by use of a BAS PWR-3 potentiostat functioning in conjunction with the CV-27 unit. The working electrode was a platinum foil (4.2 × 2.2 cm), the reference electrode was as described above and the auxiliary electrode a platinum coil isolated from the test solution with a Vycor disk.

Carbon, hydrogen and nitrogen analysis data were obtained from Regional Sophisticated Instrumentation Centre, Central Drug Research Institute (RSIC, CDRI), Lucknow as a technical service; after destruction of organic matter with concentrated H_2SO_4 followed by H_2O_2, uranium was analysed titrimetrically in each sample.[16]

X-Ray Crystallography.—Crystal data and additional details of the data collection and refinement for complex **3** are summarized in Table 1. The intensities were corrected for Lorentz and polarization effects. An absorption correction was made by the empirical ψ-scan method (correction factors 0.57–1.00).[17] The structure was solved by Patterson and Fourier methods using the SHELXTL PLUS program.[17,18] Least-squares refinement with non-hydrogen atoms treated anisotropically and hydrogen atoms at calculated positions converged to $R = 0.038$ and $R' = 0.036$ for 2818 reflections. A final electron-density map displayed some density in the vicinity of the uranium atom which is quite normal. Scattering factors for neutral atoms and anomalous disperson corrections were taken from refs. 19–21. All calculations were performed on a VAX 8650 computer system. Atomic coordinates are listed in Table 2, selected interatomic distances and angles in Table 3.

Additional material available from the Cambridge Crystallographic Data Centre comprises H-atom coordinates, thermal parameters and remaining bond lengths and angles.

Results and Discussion

Structure of $[UO_2(van\text{-}L\text{-}his)(bipy)]{\cdot}MeOH{\cdot}H_2O$.—This complex crystallizes in the triclinic space group $P\bar{1}$. The ORTEP[22] diagram showing the atom-numbering scheme is given in Fig. 1. The molecule is centred on seven-co-ordinate uranium in pentagonal-bipyramidal geometry. The phenoxide oxygen, imine nitrogen and one of the carboxyl oxygen atoms of the tridentate imine acid together with the two nitrogen atoms of 2,2′-bipyridyl, occupy the five corners of the equatorial co-ordination pentagon. Binding by the uranyl oxygen atoms in the two apical sites completes the pentagonal bipyramid. The two nitrogen atoms of bipy have different U–N bond lengths.[23] The axis of the C(3)–C(4) bond linking the imidazole ring is oriented in a similar fashion as in another β-aryl amino acid derived system.[8]

The O–U–O axis shows a 3.6° deviation from linearity and the puckering of the equatorial chelate rings may be visualized schematically with the help of a Darling model and the bond

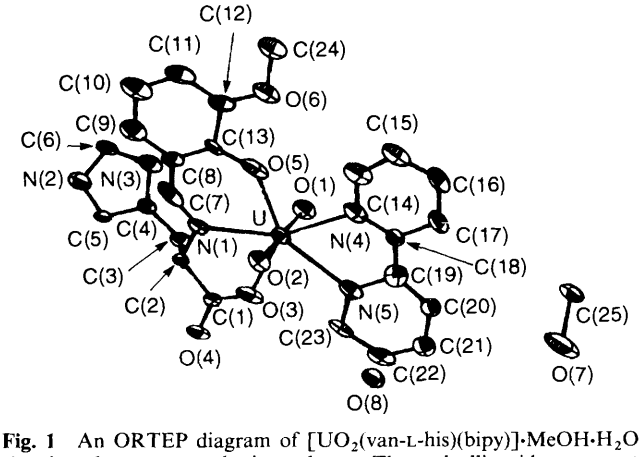

Fig. 1 An ORTEP diagram of $[UO_2(van\text{-}L\text{-}his)(bipy)]{\cdot}MeOH{\cdot}H_2O$ showing the atom-numbering scheme. Thermal ellipsoids represent 40% probability

angle data in Table 3.[24] For example, with respect to the O(1)-U axis the carboxyl oxygen and azomethine nitrogen atoms are 4.2–4.3° below the equatorial plane and the phenoxide oxygen atom is 0.9° above it.

IR Spectra.—The strong broad band of K(Hvan-L-his)·2H_2O and K(Hsal-L-his) at 1240–1231 cm^{-1} [δ(OH) + ν(C–O) mode] due to the phenolic OH group is absent in the IR spectra of the corresponding complexes; the related ν(C–O) mode (phenoxide group) appears around 1220–1210 cm^{-1}.[25,26] The ν(CH=N) vibration of the free imine acid around 1635 cm^{-1} is lowered (by 25–20 cm^{-1}) on co-ordination in all cases.[27,28] The ν_{asym} and ν_{sym} absorptions of the CO_2 group appear around 1600–1590 and 1410–1400 cm^{-1} respectively and the Δν values (*ca.* 190 cm^{-1}) indicate the presence of a unidentate CO_2 group.[25,29] The presence of dianionic tridentate aldimine residues in these complexes can be inferred. Complexes **2**–**6** attain an equatorial co-ordination number of five; for **1** an equatorial co-ordination number of six is possibly achieved (Scheme 1).

The asymmetric stretching frequency (ν_3) of the UO_2^{2+} entity occurs as a sharp band usually accompanied by a shoulder (Table 4); its doubly degenerate bending frequency (ν_2), which is usually split, appears in the region 268–256 cm^{-1} as a prominent peak, associated with shoulders.[30,31]

NMR Spectra.—Table 5 lists the proton signals of the dominant conformers of the ligands as well as those of the pertinent complexes, along with the $\Delta(=\delta_{complex} - \delta_{ligand})$ values for the latter. These assignments are based mostly on their ^1H–^1H correlation spectroscopy (COSY) data (NMR spectra); Figs 2 and 3 typify some of them. The populations of two-dimensional conformers (Table 5) have been evaluated from the time-averaged ^1H NMR spectra. Some of the important coupling constants estimated from first-order analysis of expanded one-dimensional spectra are mentioned in the text.[2]

As shown in Scheme 2, K(Hvan-L-his)·2H_2O consists of the

Table 1 Details of crystal and refinement data [UO_2(van-L-his)(bipy)]·MeOH·H_2O

Formula	$C_{25}H_{27}N_5O_8U$
M	763.54
Crystal system	Triclinic
Space group	*P*1
a/Å	7.817(4)
b/Å	9.181(6)
c/Å	10.801(12)
α/°	92.01(7)
β/°	103.51(7)
γ/°	114.18(5)
U/Å^3	680.1(5)
Z	1
D_m, D_c/Mg m^{-3}	1.85, 1.864(4)
F(000)	368
Diffractometer	Nicolet P3
Monochromator	Graphite
Crystal size/mm	0.25 × 0.20 × 0.15
Radiation	Mo-Kα(λ 0.710 69 Å)
μ(Mo-Kα)/mm^{-1}	6.02
Orientation reflections	15
2θ range/°	9.0–20.4
T/°C	20
Scan method, speed/° min^{-1}	ω, 2–25
h, *k*, *l* ranges	Minimum 0, −11, −13; maximum 9, 10, 13
Measured 2θ range/°	3.0–53.0
Check reflections, variation (%)	2, 3
No. measured reflections	2881
Observed reflections [$F_o > 5\sigma(F_o)$]	2818
R	0.038
R' [w = $1/\sigma^2(F_o)$]	0.036
Maximum Δ/σ	0.95
Maximum, minimum ρ in Δ*F* map/e Å^{-3}	3.32, −1.67

Table 3 Selected interatomic distances (Å) and angles (°) for [UO_2(van-L-his)(bipy)]·MeOH·H_2O

U–O(1)	1.761(18)	O(5)–C(13)	1.335(44)
U–O(2)	1.777(16)	N(1)–C(2)	1.470(13)
U–O(3)	2.339(9)	N(1)–C(7)	1.241(46)
U–O(5)	2.208(12)	N(4)–C(18)	1.349(24)
U–N(1)	2.564(12)	N(5)–C(19)	1.430(36)
U–N(4)	2.555(11)	C(1)–C(2)	1.594(28)
U–N(5)	2.595(15)	C(7)–C(8)	1.412(30)
O(3)–C(1)	1.226(24)	C(8)–C(13)	1.302(37)
O(4)–C(1)	1.220(16)	C(18)–C(19)	1.463(37)
O(1)–U–O(2)	174.8(7)	N(1)–U–N(4)	153.1(4)
O(3)–U–O(5)	135.7(4)	N(1)–U–N(5)	143.8(4)
O(3)–U–N(1)	65.0(4)	N(4)–U–N(5)	62.8(4)
O(5)–U–N(1)	70.7(4)	O(3)–C(1)–O(4)	128.4(21)
O(1)–U–O(3)	94.7(5)	N(2)–C(5)–C(4)	109.6(10)
O(2)–U–O(3)	89.6(5)	N(3)–C(4)–C(5)	106.8(13)
O(1)–U–O(5)	88.8(7)	N(3)–C(6)–N(2)	108.5(12)
O(1)–U–N(1)	94.8(7)	N(3)–C(4)–C(3)	131.3(12)

Table 2 Atomic coordinates (× 10^4) for [UO_2(van-L-his)(bipy)]·MeOH·H_2O

Atom	*x*	*y*	*z*	Atom	*x*	*y*	*z*
U(1)	0	0	0	C(7)	−3405(60)	1512(35)	−596(28)
O(1)	1330(26)	980(21)	−1072(14)	C(8)	−2433(18)	2833(13)	409(11)
O(2)	−1136(19)	−927(17)	1191(15)	C(9)	−3291(29)	3859(21)	637(20)
O(3)	−2424(16)	−2100(12)	−1574(11)	C(10)	−2297(26)	5182(18)	1611(16)
O(4)	−5295(14)	−3434(10)	−2971(9)	C(11)	−431(24)	5525(16)	2325(13)
O(5)	392(15)	2373(12)	859(10)	C(12)	493(21)	4585(14)	2095(11)
O(6)	2298(16)	4802(13)	2741(10)	C(13)	−638(50)	3183(32)	1024(31)
O(7)	7843(22)	−3837(17)	5413(20)	C(14)	4093(43)	1988(29)	2568(21)
O(8)	474(18)	−5482(14)	−3998(12)	C(15)	5732(24)	2526(20)	3478(14)
N(1)	−2999(14)	468(11)	−1043(10)	C(16)	6780(21)	1638(22)	3515(14)
N(2)	−7027(22)	2440(17)	−3761(20)	C(17)	6007(19)	218(19)	2639(14)
N(3)	−3882(18)	3014(14)	−3278(12)	C(18)	4196(19)	−218(18)	1721(14)
N(4)	3207(16)	692(14)	1702(10)	C(19)	3452(49)	−1668(41)	779(30)
N(5)	1542(16)	−2021(13)	−6(10)	C(20)	4187(20)	−2739(18)	716(16)
C(1)	−3988(31)	−2241(20)	−2264(17)	C(21)	3203(30)	−4132(24)	−114(22)
C(2)	−4420(16)	−694(15)	−2171(12)	C(22)	1376(25)	−4482(18)	−928(14)
C(3)	−4228(18)	67(13)	−3413(11)	C(23)	448(59)	−3386(40)	−923(37)
C(4)	−4897(16)	1383(13)	−3489(10)	C(24)	3314(25)	6130(20)	3770(14)
C(5)	−6840(17)	1055(12)	−3783(14)	C(25)	9032(19)	−2364(16)	5452(16)
C(6)	−5231(18)	3660(12)	−3421(12)				

Table 4 Analytical[a] and physical data for the dioxouranium(VI) complexes

Complex (colour)	Analysis (%) C	H	N	U	TGA, Total weight loss (%)[a,b]	$\tilde{\nu}_3$/cm^{-1}; F_{UO}/mdyn Å^{-1},[c] R_{UO}/Å of UO_2^{2+}	λ_{max}/nm (log ε/ dm^3 mol^{-1} cm^{-1})[d]
1 $K_2[UO_2(van\text{-}L\text{-}his)_2]\cdot 4H_2O$ (Dark red)	33.8 (33.8)	3.5 (3.8)	7.3 (8.4)	25.3 (23.9)	63.5 (64.9)	895 (br); 6.66, 1.74	224(br)(4.72),265(br)(4.37), 340(sh)(3.86),404(sh)(3.36), 497 (sh) (2.81)
2 $[UO_2(van\text{-}L\text{-}his)(bipy)]\cdot 3H_2O$[e] (Deep brown)	36.7 (37.6)	3.3 (3.8)	10.1 (9.1)	29.7 (31.0)	65.7 (64.8)	919, 908 (sh); 6.94, 1.74	231 (4.59), 277 (br) (4.36), 325(sh)(3.61),400(sh)(3.17), 485 (sh) (2.71)
3 $[UO_2(van\text{-}L\text{-}his)(bipy)]\cdot MeOH\cdot H_2O$ (Deep brown)	38.4 (39.3)	3.2 (3.5)	8.2 (9.2)	30.1 (31.2)	65.1[f] (65.4)	910, 897 (sh); 6.79, 1.74	231 (4.61), 277 (br) (4.38), 325(sh)(3.62),400(sh)(3.19), 485 (sh) (2.74)
4 $[UO_2(van\text{-}L\text{-}his)(phen)]\cdot H_2O$ (Deep brick-red)	41.5 (41.3)	3.2 (3.3)	8.9 (9.3)	32.2 (31.5)	62.5 (64.2)	913; 6.93, 1.74	224 (sh) (4.80), 229 (4.82), 263 (4.57), 330 (sh) (3.67), 400 (3.10), 495 (2.65)
5 $[UO_2(sal\text{-}L\text{-}his)(bipy)]\cdot 2H_2O$ (Brick red)	37.4 (38.4)	3.0 (3.2)	8.9 (9.7)	32.6 (33.1)	62.4 (62.5)	914, 898 (sh); 6.82, 1.74	214(sh)(4.60),229(sh)(4.57), 275(br)(4.28),340(sh)(3.56), 390(sh)(3.11),475(sh)(2.56)
6 $[UO_2(sal\text{-}L\text{-}his)(phen)]\cdot 4H_2O$[e] (Reddish orange)	38.8 (38.5)	2.9 (3.4)	10.1 (9.0)	30.8 (30.6)	65.6 (65.3)	913 (sh), 905; 6.87, 1.74	225 (sh) (3.86), 229 (3.86), 262 (3.59), 330 (sh) (2.78), 385(sh)(3.16),475(sh)(2.61)

[a] Calculated values in parentheses. [b] In air, heating rate *ca.* 7 °C min^{-1}, up to 720 °C; final residue U_3O_8 except for complex **1** giving an orange diuranate. [c] dyn = 10^{-5} N. [d] In methanol. For K(Hvan-L-his)·2H_2O: 225(sh)(log ε 4.17), 254 (br) (3.57), 279 (br) (3.78) and 415 nm (3.02). For K(sal-L-his): 215 (sh) (log ε 4.19), 255 (br) (3.57), 275 (br) (3.51), 320 (sh) (3.02) and 382 nm (2.76). [e] The corresponding complexes containing the D-histidine residue was synthesised and characterized in the usual way. [f] Complete elimination of H_2O and MeOH only occurs at *ca.* 175 °C.

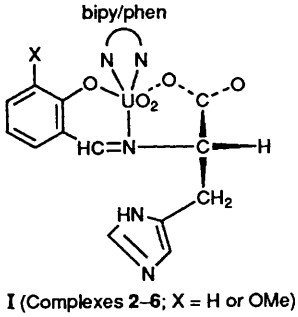

I (Complexes **2**–**6**; X = H or OMe)

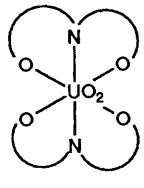

II (Complex **1**; ONO set = van -L -his^{2-})

Scheme 1

dominant conformer **III** (Table 5) and a smaller contribution from the other one, arising from anticlockwise rotation about the C_α–C_β bond; the additional signals for the latter conformer appear at δ 7.48 (CH=N), 5.23 ($H^{4'}$) and 3.71 (C^5–OCH_3). The ^{1}H NMR spectrum of K(Hsal-L-his) also indicates the presence of two conformers with two sets of signals for the CH=N (δ 7.55 and 7.71) and $H^{4'}$ (δ 5.56 and 5.25) protons. The CD spectral data (a negative Cotton effect at 315 nm, as discussed later) for K(Hsal-L-his) (obtained *in situ*) are consistent with the assignment of **III** (Scheme 2) as the major conformer of these compounds (Table 5).[3] The complete two-dimensional ^{1}H–^{1}H correlation spectrum of K(Hvan-L-his)·2H_2O indicates that protons H_{β_1}, H_{β_2} and H_α are mutually connected to each other by cross-peaks;[2] both H_{β_1} and H_{β_2} are related by cross-peaks to $H^{4'}$ (δ 5.05) which in turn is connected by off-diagonal peaks to $H^{2'}$ (δ 6.81). Cross-peaks also indicate the spin–spin interation between the C^5–OCH_3 group (δ 3.68) and H^4 (δ 6.83) and the latter in turn is related by off-diagonal peaks to H^3 (δ 6.68). The ligands possess three spin systems, *e.g.* the ABX pattern of the H_{β_1}, H_{β_2}, H_α protons, the AA'BB' [K(Hsal-L-his)] or ABC [K(Hvan-L-his)·2H_2O] pattern of the aromatic ring of the aldehyde residue and the imidazole-ring protons ($H^{2'}$ and $H^{4'}$ mostly appear as singlets). In addition, the presence of a couple of conformers usually makes difficult the straightforward interpretation of these one-dimensional spectra.[1,2]

On co-ordination of the imine acids to the UO_2^{2+} entity some interesting changes occur, *e.g.* the contributions of the major conformers increase significantly; the ^{1}H NMR spectra of some of these complexes are dominated essentially by one conformer (Table 5). Secondly, the differences in positions of the above-mentioned spin systems are enhanced to a considerable extent, *e.g.* in Fig. 2 the range of the H_α, H_{β_1} and H_{β_2} signals increases from δ 2.56–3.18 to 3.11–5.14 on complex formation. These factors make proton identification easier in spite of the inherent complexity induced by the presence of the chiral centre.[25] The complete ^{1}H–^{1}H COSY of complex **2** (Fig. 3) shows interactions among not only the different types of aromatic protons of the bipy, imidazole and benzene rings but also that of the CH=N proton with both H^2 and H_α.[12] Revelation of this long-range interaction between the CH=N and H_α protons is the most significant aspect of this two-dimensional NMR study, because the corresponding spectrum of K(Hvan-L-his)·2H_2O does not indicate this particular spin interaction. The ^{1}H–^{1}H COSY of [UO_2(van-D-his)(bipy)]·3H_2O also shows this long-range spin interaction.

The Δ values in Table 5 reveal certain important points. The protons situated around the immediate co-ordination zone (*e.g.* H_α and CH=N) are deshielded by δ 1.90–1.20; most of the other protons undergo smaller deshielding (*e.g.* up to δ 0.58 for H_{β_1}, H_{β_2} and H^4). The notable exception is the bipy/phen ring protons, which almost offset this trend, the extent of deshielding being δ 0.11–0.07. X-Ray data (Table 3) for complex **3** indicate that the heterocyclic nitrogen atoms are almost as equally strongly co-ordinated (σ bonding) as is the azomethine (CH=N) nitrogen atom (with Δ = 1.59). Evidently electron density has drifted into the bipy ring to cause this upfield shift of *ca.* δ 1.50 [δ 1.58–0.07 (or 0.11) = δ 1.51 or 1.47], of its ring protons, through

Table 5 Proton NMR chemical shifts (δ, internal $SiMe_4$) for major conformers of the ligands and those of the corresponding dioxouranium(VI) complexes, $\Delta(=\delta_{complex}-\delta_{ligand})$ values and conformer populations

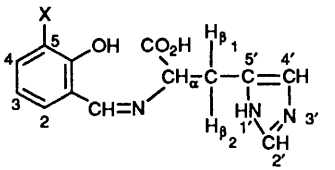

H_2sal-L/D-his X = H
H_2van-L/D-his X = OMe

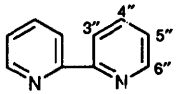

bipy

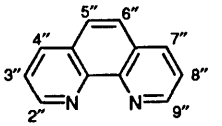

phen

Compound[a] [conformer populations (%)]		Amino acid			Aldehyde					Imidazole[b]		bipy, phen[c]			
		H_{β_1}	H_{β_2}	H_α	CH=N	C^5–OCH_3	H^2	H^3	H^4	$H^{2'}$	$H^{4'}$	$H^{6''}$	$H^{5''}$	$H^{4''}$	$H^{3''}$
												$H^{2''}$, $H^{9''}$	$H^{3''}$, $H^{8''}$	$H^{4''}$, $H^{7''}$	$H^{5''}$, $H^{6''}$
K(Hvan-L-his)·$2H_2O$[d] (89, 11)		2.56 (br d)	2.84 (br d)	3.18 (q)	7.29 (s)	3.58 (s)	6.77 (m)	6.68 (t)	6.83 (m)	6.81 (d)	5.05 (br s)	—	—	—	—
$K_2[UO_2$(van-L-his)$_2]$·$4H_2O$[d] (71, 19, 10)		2.89 (t)	3.30 (d)	5.04 (d)	7.26 (s)	3.91 (s)	6.88 (m)	6.52 (m)	7.15 (m)	8.45 (s)	7.68 (s)	—	—	—	—
	Δ	0.33	0.46	1.86	−0.03	0.23	0.11	−0.16	0.32	1.64	2.63				
$[UO_2$(van-L-his)(bipy)]·$3H_2O$[d] (95, 5)		3.11 (q)	3.41 (q)	5.14 (q)	8.88 (s)	3.93 (s)	7.04 (q)	6.60 (t)	7.22 (q)	8.86 (sh)	7.16 (br s)	8.70 (br s)	7.46 (br s)	7.96 (t)	8.39 (br d)
	Δ	0.55	0.57	1.96	1.59	0.27	0.25	−0.08	0.39	2.05	2.11	0.07	0.11	0.11	0.08
$[UO_2$(van-D-his)(bipy)]·$3H_2O$[d] (98, 2)		3.06 (q)	3.33 (q)	5.08 (q)	8.88 (s)	3.87 (s)	7.03 (d)	6.58 (t)	7.22 (d)	8.88 (s)	7.17 (s)	8.69 (d)	7.45 (q)	7.95 (sxt)	8.39 (d)
	Δ	0.54	0.49	1.90	1.59	0.19	0.26	−0.10	0.36	2.07	2.12	0.06	0.10	0.10	0.08
K(Hsal-L-his)[e] (77, 23)		2.84[f]	3.10[f]	3.72 (q)	7.55 (s)	—	g	g	g	6.87 (s)	5.56 (s)	—	—	—	—
$[UO_2$(sal-L-his)(phen)]·$4H_2O$[d] (essentially one form)		3.11 (q)	3.40 (q)	5.15 (q)	8.87 (s)	—[h]	6.96 (d)	6.65 (t)	7.43 (q)	8.76 (d)	7.13 (s)	9.10 (q)	7.79 (q)	8.52 (q)	8.02 (s)
	Δ	0.27	0.30	1.43	1.32	—	—	—	—	1.89	1.87	0	0.08	0.06	0.05
$[UO_2$(sal-D-his)(phen)]·$2H_2O$[d] (essentially one form)		3.07 (q)	3.39 (q)	5.11 (q)	8.78 (s)	—[i]	6.95 (d)	6.64 (t)	7.40 (q)	8.55 (d)	7.02 (s)	9.11 (q)	7.79 (q)	8.51 (q)	8.01 (s)
	Δ	0.23	0.29	1.39	1.23	—	—	—	—	1.68	1.76	0.01	0.08	0.05	0.04

[a] Data at 300 MHz except those for K(Hsal-L-his) at 100 MHz. s = Singlet, d = doublet, t = triplet, q = quartet, sxt = sextet, spt = septet, m = multiplet, br = broad, sh = shoulder. [b] The $H^{1'}$ (NH) signal could not be properly identified. [c] Values for the proton of free bipy and phen have been taken from ref. 32. [d] In Me_2SO. [e] In D_2O. [f] Complex AB pattern, unresolved at 100 MHz. [g] Signals of H^{2-5} could not be resolved at 100 MHz. [h] H^5 at δ 7.76 (hpt). [i] H^5 at δ 7.54 (hpt).

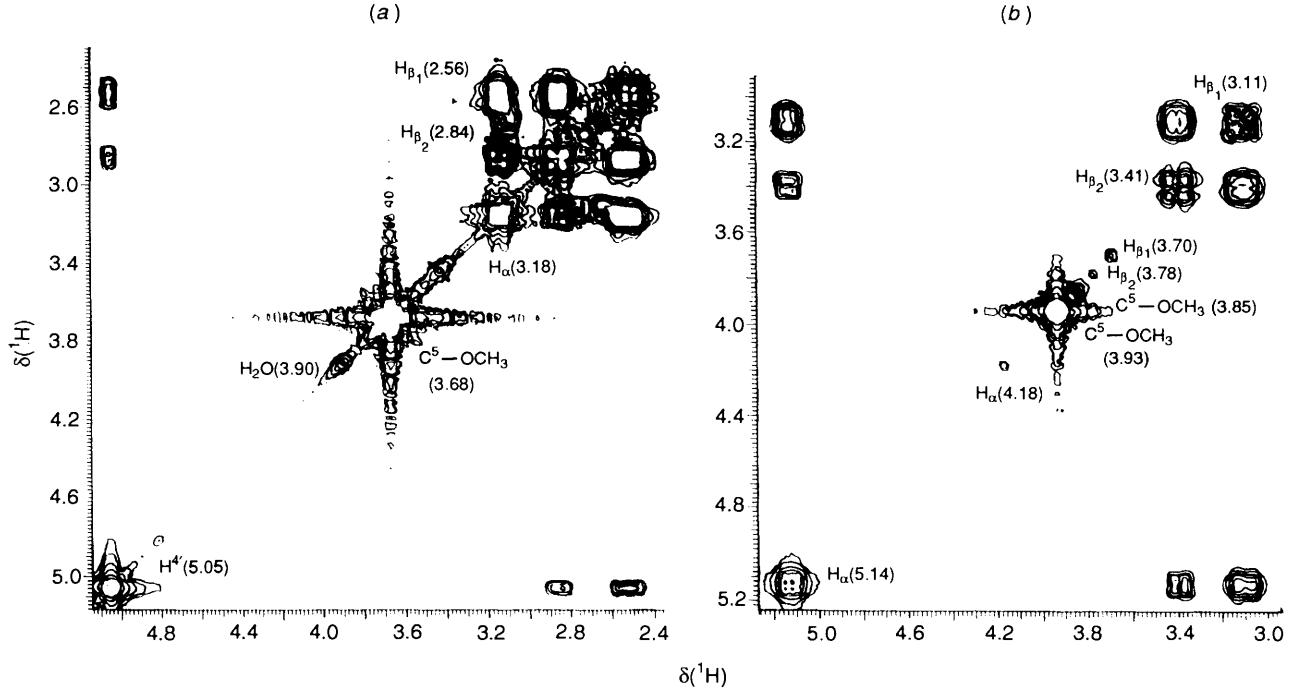

Fig. 2 Two-dimensional ^1H–^1H COSY in dimethyl sulfoxide of (*a*) K(Hvan-L-his)·2H_2O (δ 5.1–2.4) and (*b*) [UO_2(van-L-his)(bipy)]·3H_2O (δ 5.2–3.0). In (*b*) the signals at δ 3.70, 3.78, 3.85 and 4.18 correspond to the minor conformer (see Table 5)

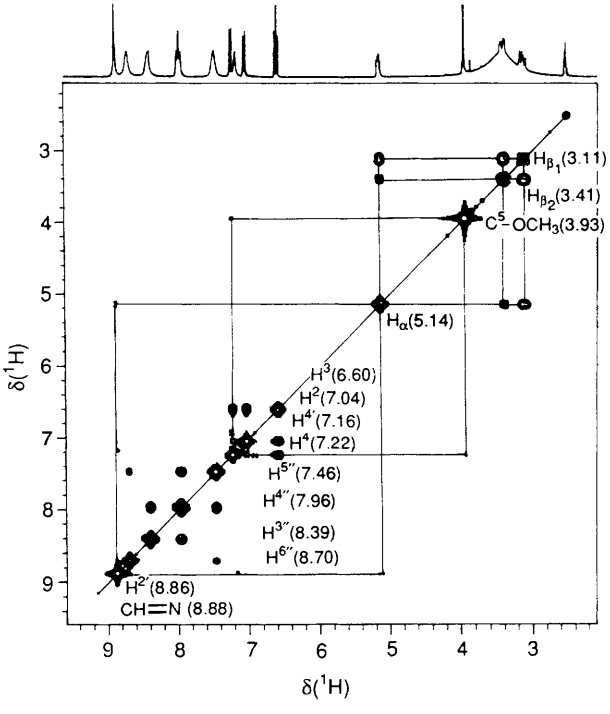

Fig. 3 Two-dimensional ^1H–^1H COSY (partly symmetrized) in dimethyl sulfoxide of [UO_2(van-L-his)(bipy)]·3H_2O (δ 9.4–2.2); see Table 5 for the proton-numbering scheme

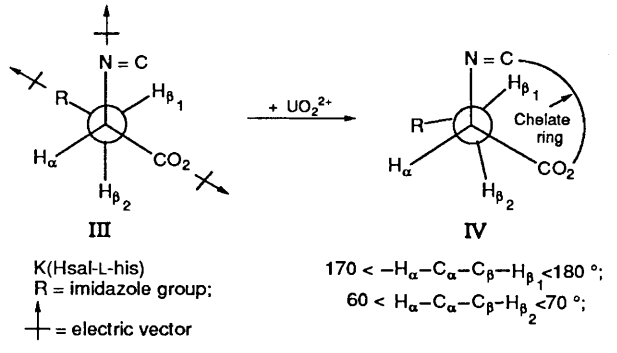

Scheme 2

M→L π bonding among the suitable uranium orbitals and the bipy π* orbitals.[33]

Among the three factors (configurational, conformational, vicinal) contributing to the optical activity of these complexes, the role of conformation is evident from the comparative ^1H NMR spectra (Fig. 4) of the two quasi-enantiomorphous complexes (Fig. 6). The differences in splitting patterns of the similar types of proton signals as well as their small differences in chemical shifts result from conformational differences (about the N–C_α and C_α–C_β bonds). Such differences lead to the observed different ellipticity values at any particular wavelength in the respective CD curves of Fig. 6; the positive and negative signs of these CD curves are determined by configurational factors.[3,8]

Comparable differences in the ^1H NMR and CD spectra, originating from conformational and configurational differences, are also observed for complex **6** and its quasi-enantiomer containing the sal-D-his^{2-} residue (Table 5).

The identification of the different proton signals (Table 5) for complex **1** is based as usual on the molecular connectivity relations, as revealed by the ^1H–^1H COSY data. This complex consists of three conformers as indicated by three different signals for each of the $H^{2'}$, $H^{4'}$ and C^5–OCH_3 protons. The azomethine proton (CH=N) signal is shielded upon co-ordination, although the IR spectral data are consistent with the presence of a co-ordinated azomethine group [the ν(CH=N) band appears at 1610 cm^{-1}]; the corresponding H_α signal is strongly deshielded (Δ = 1.86). An intramolecular ring-current effect is responsible for this exceptional shielding.

Apart from this occasional major participation of the intramolecular ring-current effect, the observed changes in chemical shift values (Δ) of the ligand protons upon chelation depend essentially on factors such as the nature of the metal–ligand bonds (*e.g.* L→M σ and M→L π types associated with deshielding/shielding effects as stated above) and magnetic anisotropy of the UO_2^{2+} entity.[34]

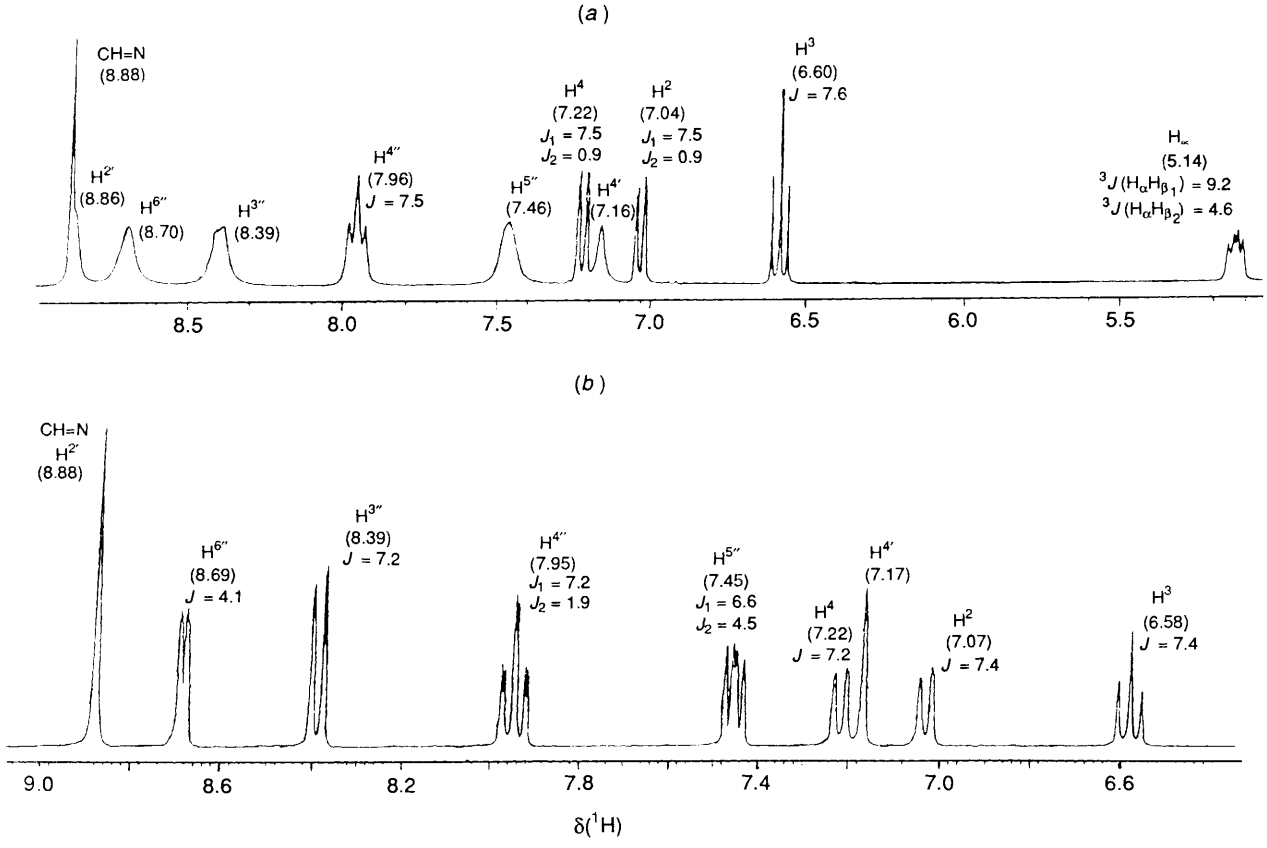

Fig. 4 Comparative ^{1}H NMR spectra (δ 9.0–5.1, J in Hz) in dimethyl sulfoxide of (*a*) $[UO_2$(van-L-his)(bipy)$]\cdot 3H_2O$ and (*b*) $[UO_2$(van-D-his)(bipy)$]\cdot 3H_2O$

The changes in chemical shift values ($\Delta\sigma_m$) for protons in the neighbourhood of the anisotropic field of the UO_2^{2+} entity, is given by $\Delta\sigma_m = \Delta x_{atomic}(1 - 3\cos^2\gamma)/3R^3$, where $\Delta x_{atomic} = -2.74 \times 10^{-34}$ m^3, R is the distance (m) of the proton from the anisotropic group and γ is the angle between a line joining the proton to the centre of the anisotropic group and the axis of symmetry of the latter.[34] From the Darling model of complex **3**, R values for the H_α and H_{β_1}/H_{β_2} protons are taken as 4.7 and 6.5 Å, along with γ values of 80 and 70°, respectively. Using the above equation, the $\Delta\sigma_m$ values are calculated to be 0.80 and 0.21 respectively. These data indicate that deshielding due to the L→M σ bonding makes a definite contribution to the observed Δ values (*e.g.* of H_α, H_{β_1}/H_{β_2}, *etc.*, Table 5).

The vicinal coupling constants $^3J_1(H_\alpha H_{\beta_1})$ and $^3J_2(H_\alpha H_{\beta_2})$ for the compounds K(Hvan-L-his)$\cdot 2H_2O$ and K(Hsal-L-his) vary around 12.3–10.4 and 3.7–4.4 Hz respectively.[2] For the corresponding dioxouranium(VI) complexes the values are 10.0–7.7 and 2.2–4.8 Hz respectively. The most important factor influencing these couplings is the dihedral angle between the C–H bonds (*e.g.* $J = 4.2 - 0.5\cos\varphi + 4.5\cos 2\varphi$ where φ is the dihedral angle).[35] Using Scheme 2 and assuming the dihedral angles (φ) H_α–C_α–C_β–H_{β_1} and H_α–C_α–C_β–H_{β_2} to be 180 and 60° for the imine acids, the above equation yields $^3J_1(H_\alpha H_{\beta_1})$ and $^3J_2(H_\alpha H_{\beta_2})$ of 9.2 and 2.5 Hz respectively. Using φ values of 170 and 70° for the corresponding complexes, the coupling constants are calculated to be 7.3 and 1.3 Hz respectively. A comparison of the calculated with the observed vicinal coupling constants indicates that the assumptions regarding the magnitudes of the dihedral angles are quite useful and may serve as guidelines for chiroptical discussions.

Electronic and CD Spectra.—Figs. 5 and 6 show some representative electronic absorption and circular dichroism (CD) spectra of these complexes; the quasi-enantiomeric nature of the CD curves in Fig. 6 stresses the importance of the absolute

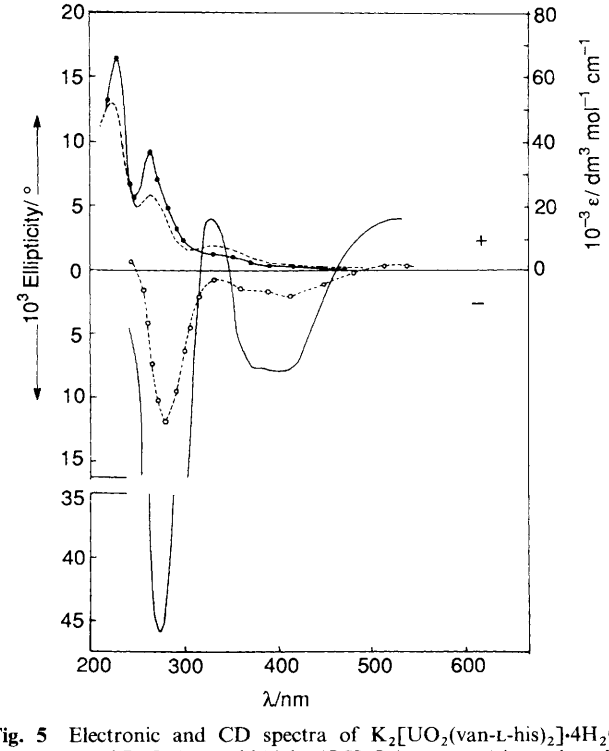

Fig. 5 Electronic and CD spectra of $K_2[UO_2$(van-L-his)$_2]\cdot 4H_2O$ (●, ——) and $[UO_2$(van-L-his)(phen)$]\cdot H_2O$ (– – – –, ○) in methanol

configuration of the amino acid residue in determining the overall chirality in such cases.[3,8]

The characteristic bands in Fig. 5 around 330 and 230 nm are assigned to π ⟶ π* transitions of the intramolecularly hydrogen-bonded *o*-vanillylidenamino chromophore (in form

V, Scheme 3).[3] The band at 265 nm for complex **1** is due to a n ⟶ π* transition of the azomethine group and gives rise to the negative Cotton effect around 275 nm (Fig. 5), through strong coupling with the π ⟶ π* transition of the CO_2 group below 210 nm.[3] The band around 260–280 nm for the base adducts is due to π ⟶ π* transitions of the bipy/phen moieties.[36] Although the free imine acid band at 400 nm is assigned to the quinonoid form **VI** (Scheme 3),[3] for the corresponding dioxouranium(VI) complexes this region of the spectra is characterized by a charge-transfer transition of comparable intensity from the equatorial ligand p_π orbitals to the 5f and/or 6d orbitals of the uranium (Fig. 5). The apical oxygen p_π ⟶ f transition within the UO_2^{2+} entity is obscured by the aforesaid strong absorption occurring in the range 350–550 nm.[30,34c,37] Nevertheless, this magnetically allowed intraoxometal transition gives rise to the relatively weak broad CD band around 500–550 nm (Figs. 5 and 6).[37,38]

The CD spectra (Figs. 5 and 6) can be divided into three distinct regions: (*i*) the 240–340 nm region, where an exciton-type band is observed (complex **1**, Fig. 5) with a negative CD maximum around 275 nm and a positive one around 330 nm; the latter band is of much reduced intensity and for some of the phen derivatives (complex **4**, Fig. 5) it is absent; (*ii*) the 340–460 nm region, which exhibits a strong broad CD band around 400 nm, due to a ligand-to-metal charge-transfer transition; it gives information on the puckering of the chelate rings;[8,37] and (*iii*) the 460–550 nm region, containing a weak broad CD maximum around 520–530 nm.[37,38]

In terms of the salicylideneamino chirality rule the decisive CD maximum around 330 nm is generated by the coupled-oscillator mechanism and two major situations may arise: (*a*) aliphatic α-amino acid derivatives where the sign of this band can be predicted from the preferred chirality that the attachment bond of the CO_2 group has with the phenyl group methine carbon in the *o*-vanillylidene/salicylidene chromophore; (*b*) α- and β-aryl-α-amino acid derivatives where the sign of this CD maximum is determined by the chirality of interaction of the *o*-vanillylidene/salicylidene chromophore with the aryl group which overshadows that with the carboxylate group.[3] In the molecular structure (Fig. 1) of complex **3** as represented using a Darling model (either **I** in Scheme 1 or **IV** in Scheme 2), the electric vectors of the aryl (left handed, negative) and carboxylate groups (right handed, positive) operate in opposite directions. The negative CD maximum at *ca.* 315 nm for the compounds possessing a L-amino acid residue, *e.g.* K(Hsal-L-his), indicates that the dominant conformer **III** (Scheme 2) possesses left-handed chirality [situation (*b*)].[3] In the spectra of the corresponding complexes this negative CD band is absent and a positive maximum appears at *ca.* 330 nm (*e.g.* for **1** and **2**, Figs. 5 and 6), indicating a greater contribution from the carboxylate group in such cases. This change of sign of the diagnostic CD band upon co-ordination may be ascribed to the change in dihedral angles in form **IV** (Scheme 2) due to steric interactions. The electric vector of the aryl group is forced away, so as to make its coupling with that of the *o*-vanillylidene/salicylidene chromophore less significant and essentially situation (*a*) prevails (right-handed chirality). The weak nature of this positive CD band around 330 nm (*e.g.* for complex **1**, Fig. 5) and its absence for some of the phen adducts (*e.g.* for complex **4**, Fig. 5) reflect the residual negative contribution from the imidazole group and the opposing electric vector contribution from the π ⟶ π* transition of the neutral donor ligand, respectively.[36] The presence of this diagnostic CD band for complex **2** (Fig. 6) may be ascribed to the fact that the two rings of the bipy moiety are slightly bent away from the molecular plane (Fig. 1), thereby neutralizing the opposing π ⟶ π* type contribution.[36]

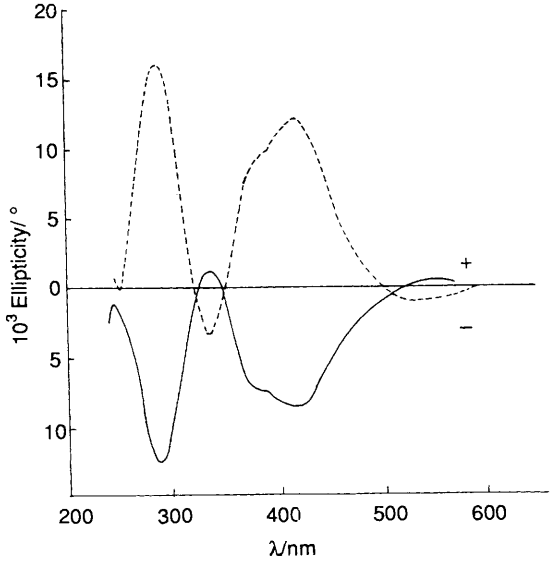

Fig. 6 The CD spectra of $[UO_2(van\text{-}L\text{-}his)(bipy)]\cdot 3H_2O$ (——) and $[UO_2(van\text{-}D\text{-}his)(bipy)]\cdot 3H_2O$ (– – – –) in methanol

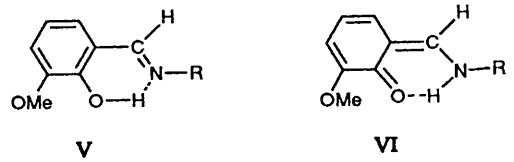

Scheme 3

Cyclic Voltammetric Studies and Conformational Effects.— Table 6 summarizes the electrochemical data and Fig. 7 shows two of the cyclovoltammogram diagrams. For each ligand system an extended cyclovoltammogram was run initially (0 to −2.0 V) to establish the limits imposed by the potential at which the ligand begins to reduce [*e.g.* for K(Hsal-L-his) E_{pc} = −1.63 V at 50 mV s^{-1}, an irreversible process] and in subsequent CV measurements the potential range was limited (−0.8 to −1.2 V) to include only that interval in which the complex itself was being reduced and oxidized. The peak system is due to the uncomplicated one-electron process UO_2^{2+} ⟶ UO_2^{+} for these complexes.[39] This assignment has been checked by controlled-potential coulometric reductions, *e.g.* $[UO_2(van\text{-}L\text{-}his)(bipy)]\cdot MeOH\cdot H_2O$ at −1.10 V *vs.* SCE which showed a consumption of 1.06 per molecule of complex, verifying the one-electron nature of the reduction wave. Most of the systems studied tended to show an increase in the cathodic and anodic peak separation as a function of scan rate corresponding to quasi-reversible behaviour. The cyclovoltammogram [Fig. 7(*a*)] of $[UO_2(van\text{-}L\text{-}his)(bipy)]\cdot MeOH\cdot H_2O$ in the scan rate (v) range 50–175 mV s^{-1} reveals the following electrochemical parameters: $E_{\frac{1}{2}}$ = −0.98 V, ΔE_p = 145 ± 15 mV and i_{pc}/i_{pa} = 1.78 ± 0.07 and a linear dependence of i_{pc} on $v^{\frac{1}{2}}$. The characteristics of the other cyclovoltammogram [Fig. 7(*b*)] at comparable scan rates are $E_{\frac{1}{2}}$ = −1.00 V, ΔE_p = 145 ± 15 mV, i_{pc}/i_{pa} = 1.77 ± 0.17 and a linear dependence of i_{pc} on $v^{\frac{1}{2}}$. The kinetic parameter (i_{pc}/i_{pa}, Table 6) characterizes the most important difference between the two quasi-enantiomers in Fig. 7. Their conformational differences as identified earlier from chiroptical studies (Figs. 4 and 6) account for the difference in electrochemical behaviour.[10]

In terms of molecular orbital theory, during electrochemical reductions the relevant half-filled highest occupied molecular orbitals (HOMOs) accept electrons and the conformational factors have a direct bearing on their energy.[10] The MO picture reveals that the twelve electrons of the UO_2^{2+} entity fill up the available bonding orbitals $[(1\sigma_g)^2(1\sigma_u)^2(\pi_u)^4(\pi_g)^4]$, leaving the δ_u, φ_u and δ_g orbitals empty.[30,33] The electrons donated by the equatorial ligands almost fill up the δ_u orbital, leaving the φ_u and δ_g orbitals suitable for participation in the observed electrochemical changes. Reduction to the UO_2^{+} state is

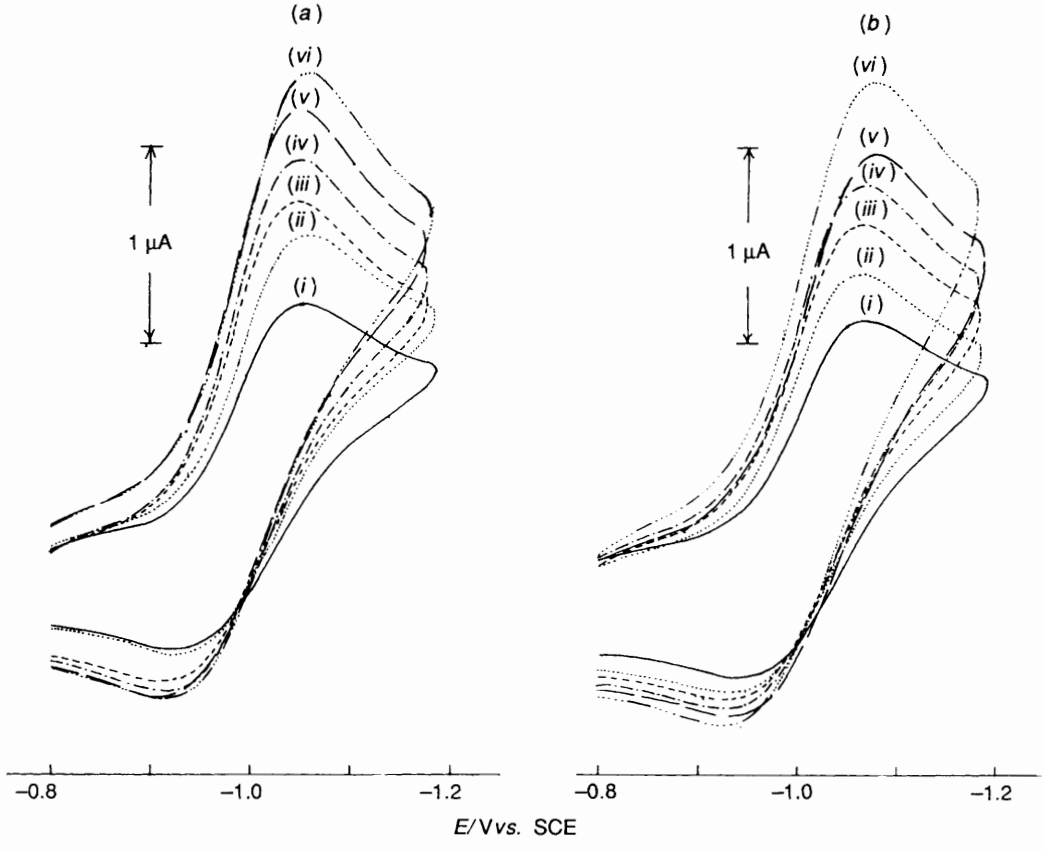

Fig. 7 Cyclic voltammograms of (*a*) $[UO_2(van\text{-}L\text{-}his)(bipy)]\cdot MeOH\cdot H_2O$ and (*b*) $[UO_2(van\text{-}D\text{-}his)(bipy)]\cdot 3H_2O$ in Me_2SO (*ca.* 1×10^{-3} mol dm^{-3}) with 0.1 mol dm^{-3} $[NBu_4][ClO_4]$. Scan rates (*i*) 50, (*ii*) 75, (*iii*) 100, (*iv*) 125, (*v*) 150 and (*vi*) 175 mV s^{-1}

Table 6 Summary of electrochemical data for the dioxouranium(VI) complexes[a]

	$UO_2^{2+} + e \rightleftharpoons UO_2^{+}$				
Complex	E_{pc}/V	E_{pa}/V	ΔE_p[b]/mV	$E_{\frac{1}{2}}$[c]/V	i_{pc}/i_{pa}
$[UO_2(van\text{-}L\text{-}his)(bipy)]\cdot MeOH\cdot H_2O$	−1.05	−0.92[d]	130	−0.98	1.76
$[UO_2(van\text{-}D\text{-}his)(bipy)]\cdot 3H_2O$	−1.07	−0.94[d]	130	−1.00	1.60
$K_2[UO_2(van\text{-}L\text{-}his)_2]\cdot 4H_2O$	−1.08	—[e]	—	—	—
$[UO_2(sal\text{-}L\text{-}his)(phen)]\cdot 4H_2O$	−1.06	−0.92[d]	140	−0.99	2.43

[a] Cyclic voltammetry *vs.* SCE at 50 mV s^{-1}, 25 °C. [b] $\Delta E_p = E_{pc} - E_{pa}$; where E_{pc} and E_{pa} are the cathodic and anodic peak potentials respectively; i_{pc} and i_{pa} are the corresponding peak currents (μA). [c] $E_{\frac{1}{2}} = 0.5\ (E_{pc} + E_{pa})$. [d] The broad anodic response becomes better defined at faster scan rates. [e] The anodic peak is poorly defined.

accompanied by an increase in size.[39] These aldimine ligands with a large R group (histidyl residue), in conjunction with bipy/phen form a compact co-ordination sphere around the VO_2^{2+} entity, so that the electroinduced stereochemical rearrangements, leading to subsequent chemical reactions, are largely prevented before the start of the reverse anodic scan.

The anodic peak of $K_2[UO_2(van\text{-}L\text{-}his)_2]\cdot 4H_2O$ is poorly defined (Table 6) and the relevant CV response is essentially an irreversible reduction process ($U^{VI} \longrightarrow U^{V}$) followed by extensive chemical reactions (*e.g.* solvolysis). In this anionic complex the UO_2^{2+} entity has hardly any scope to shed the accumulated charge on it through M→L π bonding with the bipy/phen moiety, as for the other complexes in Table 6.

Conclusion

In the mixed mononuclear complexes **2**–**6** the diamagnetic UO_2^{2+} entity attains a pentagonal-planar co-ordination geometry. It imposes a unique restriction on the chiral aldimine ligands which thereby retain their absolute configurations (Fig. 6) and helps in several ways the interpretation of their NMR spectra; *e.g.* the contribution from the major conformer increases significantly, the different proton signals are well spread out (Fig. 2) and above all the two-dimensional NMR data reveal the different spin–spin interactions (Fig. 3). Of the three distinct portions in the CD spectra (Figs. 5 and 6) the region below 350 nm is valuable in determining the conformation about the N–C_α bond as well as the contributions (electric vectors) from the adjacent chromophores to the diagnostic band at *ca.* 330 nm; the middle region (350–500 nm) reflects the puckering of the chelate rings; and the third portion above 500 nm reflects the fact that the absolute configuration of the amino acid residue determines the chirality (vicinal effect) of the π ⟶ f charge-transfer transition within the UO_2^{2+} entity.

The CV response of these complexes is influenced by several factors, *e.g.* the conformational properties of the chelated ligands, the equatorial co-ordination number, compactness of the equatorial donor set and the possibility of M→L π bonding. For complexes with scope for such π bonding the chelate rings are capable of adjusting with the size increase accompanying

cathodic reduction and this corresponds to quasi-reversible CV behaviour. Even in such cases the ligand conformational differences can influence in a small but definite way the metal-centred electron-transfer process.

Acknowledgements

We thank the University Grants Commission, New Delhi, for a teacher fellowship (to S. P.), the Department of Science and Technology, New Delhi, for assistance in the form of a research project (for P. S. R.), RSIC, CDRI, Lucknow for microanalytical data and CD spectra and RSIC, Indian Institute of Technology, Bombay for Fourier-transform NMR spectra. Some of the IR spectra (CsI discs) were recorded by the RSIC, North Eastern Hill University, Shillong. Thanks are also due to Dr. S. Das, Chemistry, North Bengal University for his help in electrochemical studies.

References

1 R. H. Holm, *Inorganic Biochemistry*, ed. G. L. Eichhorn, Elsevier, New York, 1975, vols. 1 and 2, ch. 31.
2 M. D. Tsai, S. R. Byrn, C. Chang, G. F. Heinz and H. J. R. Weintraub, *Biochemistry*, 1978, **17**, 3177.
3 H. E. Smith, *Chem. Rev.*, 1983, **83**, 359.
4 I. I. Mathews and H. Manohar, *J. Chem. Soc., Dalton Trans.*, 1991, 2289.
5 H. C. Dunathan, *Proc. Natl. Acad. Sci. USA*, 1966, **55**, 712; *Adv. Enzymol.*, 1971, **35**, 79.
6 K. Korhonen and R. Hämäläinen, *Acta Chem. Scand., Ser. A*, 1979, **33**, 569.
7 H. M. Dawes, J. M. Waters and T. N. Waters, *Inorg. Chim. Acta*, 1982, **66**, 29.
8 S. Panchanan, M. C. Saha, R. Roy and P. S. Roy, presented at the 4th Symposium on Modern Trends in Inorganic Chemistry, Central Salt and Marine Chemicals Research Institute, Bhavnagar, October 1991.
9 L. Casella and M. Gullotti, *Inorg. Chem.*, 1981, **20**, 1306; L. Casella, M. Gullotti, A. Pasini, G. Ciani, M. Manassero and A. Sironi, *Inorg. Chim. Acta*, 1978, **26**, L1.
10 M. M. Bernardo, R. R. Schroeder and D. B. Rorabacher, *Inorg. Chem.*, 1991, **30**, 1241; P. Osvath and A. G. Lappin, *J. Chem. Soc., Chem. Commun.*, 1986, 1056; C. S. J. Chang and J. H. Enemark, *Inorg. Chem.*, 1991, **30**, 683; W. Hubber and K. Müllen, *Acc. Chem. Res.*, 1986, **19**, 300.
11 J. Frelek, Z. Majer, A. Perkowska, G. Snatzke, I. Vlahov and U. Wagner, *Pure Appl. Chem.*, 1985, **57**, 441.
12 U. Casellato, P. Guerriero, S. Tamburini, P. A. Vigato and R. Graziani, *J. Chem. Soc., Dalton Trans.*, 1990, 1533.
13 R. J. Sundberg and R. B. Martin, *Chem. Rev.*, 1974, **74**, 471; F. Schneider, *Angew. Chem., Int. Ed. Engl.*, 1978, **17**, 583; A. S. Brill, *Transition Metals in Biochemistry*, Springer, New York, 1977, ch. 2.
14 D. T. Sawyer and J. L. Roberts, jun., *Experimental Electrochemistry for Chemists*, Wiley, New York, 1974.
15 A. I. Vogel, *Text Book of Practical Organic Chemistry*, 4th edn., Longman, London, 1978; D. F. Shriver and M. A. Drezdzon, *The Manipulation of Air-sensitive Compounds*, 2nd edn., New York, 1986.
16 G. Charlot and D. Bezier (transl. R. C. Murray), *Quantitative Inorganic Analysis*, Methuen, London, 1957, pp. 309, 619.
17 Program Package, Nicolet XRD Corporation, Cupertino, CA, 1980; G. M. Sheldrick, SHELXTL PLUS, Program package of structure solution and refinement, Version 4.2, Siemens Analytical Instruments Inc., Madison, WI, 1990.
18 G. M. Sheldrick, *Acta Crystallogr., Sect. A*, 1990, **46**, 467.
19 D. T. Cromer and D. Liberman, *J. Chem. Phys.*, 1970, **53**, 1891.
20 D. T. Cromer and J. B. Mann, *Acta Crystallogr., Sect. A*, 1968, **24**, 321; R. F. Stewart, E. R. Davidson and W. T. Simpson, *J. Chem. Phys.*, 1965, **42**, 3175.
21 *International Tables for X-Ray Crystallography*, Kynoch Press, Birmingham, 1974, vol. 4.
22 C. K. Johnson, ORTEP, Report ORNL-5138, Oak Ridge National Laboratory, Oak Ridge, TN, 1976.
23 A. G. Orpen, L. Brammer, F. H. Allen, O. Kennard, D. G. Watson and R. Taylor, *J. Chem. Soc., Dalton Trans.*, 1989, S1.
24 Darling Flexible Stereochemistry Molecular Model, Stow, OH, 1986.
25 R. M. Silverstein, G. C. Bassler and T. C. Morrill, *Spectrometric Identification of Organic Compounds*, 4th edn., Wiley, New York, 1981.
26 L. J. Bellamy, *The Infrared Spectra of Complex Molecules*, 3rd edn., Chapman and Hall, London, 1975.
27 D. E. Fenton, U. Casellato, P. A. Vigato and M. Vidali, *Inorg. Chim. Acta*, 1984, **95**, 187.
28 U. Casellato, D. Fregona, S. Sitran, S. Tamburini, P. A. Vigato and D. E. Fenton, *Inorg. Chim. Acta*, 1985, **110**, 181.
29 G. B. Deacon and R. J. Phillips, *Coord. Chem. Rev.*, 1980, **33**, 227.
30 S. P. McGlynn, J. K. Smith and W. C. Neely, *J. Chem. Phys.*, 1961, **35**, 105; S. P. McGlynn and J. K. Smith, *J. Mol. Spectrosc.*, 1961, **6**, 164; R. G. Denning, T. R. Snellgrove and D. R. Woodwork, *Mol. Phys.*, 1979, **37**, 1109.
31 C. L. Garg and K. V. Narasimham, *Spectrochim. Acta, Part A*, 1971, **27**, 863.
32 S. Castellano, H. Gunther and S. Ebersole, *J. Phys. Chem.*, 1965, **69**, 4166; J. D. Miller and R. H. Prince, *J. Chem. Soc.*, 1965, 4706.
33 L. Cattalini, U. Croatto, S. Degetto and E. Tondello, *Inorg. Chim. Acta Rev.*, 1971, **5**, 19.
34 (*a*) T. H. Siddall and C. A. Prohaska, *Inorg. Chem.*, 1965, **4**, 783; (*b*) J. D. Pedrosa and V. M. S. Gil, *J. Inorg. Nucl. Chem.*, 1974, **36**, 1803; (*c*) B. I. Kim, C. Miyake and S. Imoto, *J. Inorg. Nucl. Chem.*, 1974, **36**, 2015.
35 J. R. Dyer, *Applications of Absorption Spectroscopy of Organic Compounds*, Prentice-Hall of India Pvt., New Delhi, 1987, pp. 116, 118.
36 B. Bosnich, *Acc. Chem. Res.*, 1969, **2**, 266.
37 A. Pasini, M. Gullotti and E. Cesarotti, *J. Inorg. Nucl. Chem.*, 1972, **34**, 3821.
38 R. Roy, M. C. Saha and P. S. Roy, *Inorg. Chim. Acta*, 1987, **129**, 265.
39 R. L. Lintvedt, W. E. Lynch and J. K. Zehetmair, *Inorg. Chem.*, 1990, **29**, 3009; P. Zanello, A. Cinquantini, P. Guerriero, S. Tamburini and P. A. Vigato, *Inorg. Chim. Acta*, 1986, **117**, 91.

Received 8*th March* 1994; *Paper* 4/01358A